Applied Catalysis B: Environmental 174–175 (2015) 85–95

Contents lists available at ScienceDirect

Applied Catalysis B: Environmental

journal homepage: www.elsevier.com/locate/apcatb

A survey of catalysts for aromatics from fast pyrolysis of biomass

Shantanu Kelkar[a,b], Christopher M. Saffron[a,c,*], Kevin Andreassi[a], Zhenglong Li[a,b], Ambareesh Murkute[b], Dennis J. Miller[b], Thomas J. Pinnavaia[d], Robert M. Kriegel[e]

[a] Department of Biosystems & Agricultural Engineering, Michigan State University, USA
[b] Department of Chemical Engineering & Materials Science, Michigan State University, USA
[c] Department of Forestry, Michigan State University, USA
[d] Department of Chemistry, Michigan State University, USA
[e] The Coca-Cola Company, 1 Coca-Cola Plaza, Atlanta, GA, USA

ARTICLE INFO

Article history:
Received 7 January 2015
Accepted 17 February 2015
Available online 19 February 2015

Keywords:
Pyrolysis
Catalyst
Zirconia
Zeolite
Red mud
Mesoporous

ABSTRACT

A comparative evaluation of ten catalysts for biomass pyrolysis was performed using poplar (DN-34) as the feedstock. Five of the catalysts consisted of HZSM-5 with different silica:alumina ratios (SAR, 23, 30, 55, 80 and 280). The other five catalysts were sulfated zirconia ($SO4^{2-}$ ZrO_2), 20% $SO4^{2-}$ ZrO_2 dispersed on a mesoporous MCM-41 silica support, Al–MSU–S alumnosilicate exhibiting a foam-like mesopore structure, Al–MSU–S aluminosilicate exhibiting wormhole mesopores, and a bauxite waste product known as red mud. Analytical pyrolysis in tandem with GC/MS showed that all of the catalysts except for HZSM-5 resulted in low aromatic chemical production. Highly acidic sulfated zirconia catalysts were not selective to aromatics and produced significant coke and non-condensable gases. Mesoporous MSU–S catalysts exhibiting high pore volume and acidity also gave high gas and coke yields. Among the HZSM-5 catalysts evaluated, those with the lowest SAR provided the highest yields of total aromatics and the lowest levels of undesired coke.

1. Introduction

Monoaromatic compounds, such as benzene, toluene, ethylbenzene and xylenes (BTEX), are used as octane boosters in gasoline and as precursors to polymers such as polyethylene terephthalate. Renewable approaches for making such aromatics from biomass will reduce the U.S. dependence on fossil petroleum and mitigate the negative impacts of climate change. One approach for depolymerizing biomass into the chemical precursors of aromatic compounds is fast pyrolysis. Biomass fast pyrolysis involves the rapid heating of biomass in the absence of oxygen at temperatures of around 500 °C. The generalized products of pyrolysis include a solid product known as char, non-condensable gases and a condensable vapor.

Catalysts aid decarboxylation and decarbonylation reactions of the vapor product to produce a new set of vapor products such as hydrocarbons, alcohols and a solid carbonaceous residue on the catalyst surface known as coke. Several researchers have used zeolite catalysts to convert carbohydrate and biomass feeds into aromatics [1–6]. Acidic catalysts enable cracking reactions that remove oxygen in the form of non-condensable gases [7]. HZSM-5 is a crystalline aluminosilicate where the ratio of silicon to aluminum in the crystal structure can be modified, affecting the hydrophilicity and the concentration of Bronsted acid sites [8]. As acids sites are necessary for cracking and aromatics production, changing the acidity of HZSM-5 was accomplished by varying the silica:alumina ratio (SAR) to study its effect.

Pyrolysis of lignocellulosic woody biomass or herbaceous crops produces lignin derivatives such as phenolic molecules [9]. The kinetic diameter of many lignin derivatives is larger than the 5.5–5.6 Å dimensions of the HZSM-5 micropores [6,10]. Therefore, although HZSM-5 is highly acidic, it is limited by low mass transfer rates for several molecules generated upon biomass pyrolysis. Mesoporous catalysts have large pores that reduce diffusion limitations and increase surface area for catalytic reactions. Surface area increases the available acidic sites for reactions that may increase conversion and reduce coke yields. Thus, mesoporous catalysts may be beneficial for generating valuable chemicals by biomass pyrolysis and many biomass–catalyst permutations warrant further study. In this regard, five additional catalysts are compared to HZSM-5 for their potential to produce aromatics; namely Al–MSU–S exhibiting foam-like mesopore structure, Al–MSU–S exhibiting wormhole mesopores, highly acidic sulfated zirconia, sulfated zirconia dispersed on mesoporous MCM-41 support and red mud, a hazardous waste from bauxite mining.

* Corresponding author at: 204 Farrall Hall, 524 S Shaw Ln, East Lansing, MI 48824, USA. Tel.: +1 517 432 7414.
E-mail address: saffronc@egr.msu.edu (C.M. Saffron).

http://dx.doi.org/10.1016/j.apcatb.2015.02.020
0926-3373/

Al–MSU–S catalysts have acidity as well as hydrothermal stability, necessary for highly corrosive applications such as fast pyrolysis [11]. Sulfated zirconia (SO_4^{2-}-ZrO_2) is an environmentally benign super acid shown to be active in a number of reactions such as isomerization, cracking, alkylation and acylation [12]. Its potential for pollution control such as selective NOx reduction has been demonstrated although its applications for upgrading pyrolysis oil have not been well explored [13]. Due to its low surface area, this catalyst has not seen many commercial applications [14]. Sulfated zirconia on the mesoporous aluminosilicate MCM-41 support is a relatively unexplored catalyst design that can provide greater surface area and catalyst porosity. Transition metal modified MCM-41 has been shown to increase selectivity for hydrocarbons and reduce oxygenates (organic molecules with oxygen functional groups such as acetic acid, glycolaldehyde, etc.) from biomass pyrolysis vapors [11,15,16]. Therefore, the preparation of sulfated zirconia supported on mesoporous MCM-41 is demonstrated and its activity in upgrading pyrolysis vapor is investigated.

To improve economic feasibility of biomass pyrolysis to aromatics, inexpensive catalysts are necessary. One such catalyst is red mud, which is produced as a waste during bauxite refining for aluminum. The disposal of red mud is an environmental concern [17,18]. Red mud is composed of many transition metal oxides, favors hydrogenation reactions and may prove to be an inexpensive catalyst for biofuel applications [17,19] .

An objective of the present study was to screen catalysts while simulating a pyrolysis process followed by catalysis. Separating the pyrolysis step from catalysis allows for better process control and easier collection of bio-char, a valuable by-product, which itself has many applications. Thus, in the present investigation, five different varieties of HZSM-5 along with five additional acidic and mesoporous catalysts are explored for producing aromatics from biomass pyrolysis. These ten catalyst varieties were selected for properties such as acidity, mesoporosity or low cost, that may help improve the efficiency of the biomass pyrolysis to aromatics process. Though prior research has explored the use of HZSM-5 for converting neat sugars [1,20], cellulose [21], lignin [22] and biomass [2,23] as feedstock, the impact of catalyst properties such as surface area and acidity has not been assessed in tandem with the use of raw biomass. Deoxygenation and aromatization activity of sulfated zirconia, red mud and Al–MSU–S and their comparison with the conventional HZSM-5 catalyst has not been studied. The present investigation begins to suture these knowledge gaps and in addition, explores and compares several varieties of HZSM-5 in terms of catalyst properties and aromatic product yields.

2. Experimental

2.1. Catalysts

ZSM-5 catalysts with the following silica–alumina ratios 23, 30, 55, 80 and 280 were obtained from Zeolyst Co. (Conshohocken, PA) in ammonium cation form. In order to obtain the acidic HZSM-5 form, the catalyst was calcined in air at 550 °C for 4 h prior to use. The properties of the catalysts, as measured by Zeolyst, were similar in surface area (400–425 m^2/g), pore size (~0.6 nm) and pore volume (~0.14 m^3/g).

The (2%) Al–MSU–S foam (henceforth referred to as foam) and (2%) Al–MSU–S worm (worm) were synthesized from zeolite beta seeds as precursors and the polymers cetyltrimethylammonium bromide (CTAB) and tallow tetramine as structure-directing agents. A detailed procedure for preparing these catalysts is described elsewhere [24,25]. Red mud was obtained from Professor Marcel Schlaf at the University of Guelph. The red mud was sourced as slurry from the Rio Tinto Alcan mining facility in Canada and contained about 50% w/w iron oxide. The slurry was water washed and dried at 120 °C [19].

Sulfated zirconia catalyst (henceforth referred to as SZ) was prepared by hydrolysis of $ZrOCl_2{\cdot}8H_2O$ with aqueous ammonia, treating with 0.5 M H_2SO_4 and calcination at 650 °C. The sulfated zirconia supported in mesoporous material (20% SO_4^{2-} ZrO_2 MCM-41, henceforth referred to as MSZ) was prepared by dispersion of $ZrOCl_2{\cdot}8H_2O$ (20% ZrO_2) on to MCM-41 support using the incipient wetness method followed by drying at 105 °C for 12 h [6]. The mixture was treated with ammonia gas leading to formation of amorphous $Zr(OH)_4$. The sample was then water washed, treated with 0.5 M of H_2SO_4 solution at room temperature for 10 min and calcined at 650 °C in air for 3 h.

2.2. Catalyst characterization

Surface area measurements and pore size distribution analysis were done by nitrogen adsorption at 78 K (−195 °C) in a Micromeritics ASAP 2010 instrument. Prior to measurements, the sample was out-gassed in the degas port of the apparatus at 220 °C for 24 h. NH_3-TPD measurements were performed by volumetric adsorption in a Micromeritics AutoChem 2910 instrument. A thermal conductivity detector and an Ametek Dycor M100M Quadrupole Mass Spectrometer were used for continuous monitoring of the desorbed NH_3. Prior to NH_3 adsorption, approximately 0.5 g of catalyst was thermally pretreated in He (99.999%) at a flow rate of 50 $cm^3\,min^{-1}$ at 410 °C for 1 h followed by cooling to ambient temperature in He. After pretreatment, each catalyst was saturated at ambient temperature with NH_3 (99.998%) at a flow rate of 50 $cm^3\,min^{-1}$ for 1 h and then subsequently purged with He (50 $cm^3\,min^{-1}$) for 2 h to remove all physisorbed NH_3. Desorption of chemisorbed NH_3 was carried out in He flow with the catalyst being heated from ambient temperature to 700 °C at a rate of 10 °C min and held for 30 min. The resulting NH_3 peak was quantified by calibrating the area using a gas standard.

2.3. Pyrolysis–GC/MS and TGA

Experiments were conducted using a microscale pyrolysis unit, CDS Pyroprobe 5250 (CDS Analytical Inc., Oxford, PA) interfaced to a Shimadzu QP-5050A gas chromatograph/mass spectrometer (Shimadzu Corp., Columbia, MD). A lignocellulosic feedstock, poplar (DN-34, *Populus x euramericana,* cv. 'Eugenei'), was used as biomass for all experiments. The poplar was dried at 60 °C to a moisture content of ~8%, ground to a particle size of less than 0.5 mm and stored at room temperature [26]. For biomass pyrolysis experiments, approximately 0.5 mg of ground biomass sample was packed between quartz wool in a quartz tube. For catalytic pyrolysis experiments, approximately 0.5 mg of biomass was packed between quartz wool. Catalyst, with a 5:1 weight ratio of catalyst to biomass, was added on both sides followed by more quartz wool to hold the sample in place. Six or more replicates of each sample were run. In a scaled-up process, pyrolysis may occur in a separate pyrolysis reactor and the vapors may be conveyed to a separate catalyst reactor. To simulate this separation between the two steps, quartz wool was used inside the sample tube. This prevented mixing of the biomass and catalyst and allowed the pyrolysis of biomass to occur first. The product vapors diffuse away from the biomass due to the helium stream inside the pyroprobe and come in contact with the catalyst for the catalysis step.

Pyrolysis proceeded by setting the pyroprobe at 650 °C (pyrolysis temperature of 500–550 °C) with a hold time of 20 s at the maximum heating rate setting of 999 °C/s. The GC used a Restek rtx-1701 column (Restek, Bellefonte, PA), 60 m × 0.25 mm with a 0.25 μm film thickness. The column gas flow was 1 cm^3/s with a split ratio of 1:100 so as to not overwhelm the mass

spectrometer. The GC oven temperature program began with a 1 min hold at 40 °C followed by heating at 8 °C/min to 270 °C. The injector and detector temperature were set at 280 °C. Identification of compounds was performed by comparing the mass spectra of the peaks with standard spectra of other compounds using the 2005 NIST library to obtain the most probable matches. Pure compounds (Sigma–Aldrich Co., St. Louis, MO) were then used to confirm the peak identities based on matching of retention times and mass spectra. Quantification was performed using external standards in acetonitrile and a four-point calibration curve. Approximately 70 compounds were identified; however, external standards were run for 20 compounds as standards were not available for the rest. When pure chemicals were not available, the quantification factor used was obtained from the standard curve of the nearest similarly structured compounds e.g., anhydrosugar compounds were quantified according to levoglucosan quantification and their combined yield was reported. The mass spectra were recorded in electron ionization mode for m/z 28–300. In separate experiments to quantify non-condensable gases (carbon oxides, hydrocarbons) and volatile aromatics, an Agilent CP Porabond-Q column, 25 m × 0.25 mm × 3 μm (Agilent Technologies, Santa Clara, CA) was used under identical experimental conditions.

The solid residue left behind after biomass pyrolysis is known as char while polymeric aromatic hydrocarbons produced on the catalyst surface during the reaction of pyrolysis vapor is known as coke. In these experiments, the char and coke yields could not be measured separately and are reported as one value. The char and coke combined value was determined from the difference of weight of the sample tube before and after pyrolysis. Char and coke quantity was further confirmed by burning off the solid pyrolysis product at 650 °C in a thermogravimetric analyzer (TGA/DSC1CH-8603 model, Mettler-Toledo, Schwerzenbach, Switzerland). Nitrogen was used as the purge gas with a flow rate of 20 mL/min. Experiments with biomass alone using the pyroprobe-GC/MS and the TGA showed that the poplar char yield was approximately 23% with low standard deviations. Therefore, the differences in the combined char and coke yield for catalytic pyrolysis reactions may be attributed to coking during the catalyst reaction.

To summarize, biomass was pyrolyzed in the pyroprobe instrument, producing char in-situ. The vapors generated diffused over a catalyst (which was packed in the same sample tube but separated from biomass by quartz wool) producing coke on the catalyst surface and vapor products. The catalytic vapor products were carried by a helium stream into a GC/MS where they were identified and quantified. After the reaction was complete, the mixed residue of char, quartz wool, catalyst and coke (deposited on catalyst surface) was combusted in the TGA. The catalyst and quartz wool were unreacted at combustion temperature while the char and coke burnt off. This loss in weight gave the total amount of char and coke. To find out the char weight alone, biomass without catalyst was pyrolyzed inside a TGA pre-set at 650 °C (to simulate the high heating rate inside the pyroprobe). The residue from this experiment was char. Thus, a weight of char from poplar pyrolysis was obtained. For the same reaction conditions and biomass, char produced would be consistent, especially since the biomass in the sample tube is separated from the catalyst. Therefore, the differences in the char + coke values may be attributed to coke generation on the catalyst surface only.

3. Results and discussion

3.1. Catalyst properties

A comparison of catalyst properties in Table 1 showed that the mesorporous MSU–S catalysts had a very high surface area of 995 m^2/g for the foam (catalyst with foam-like mesoporous structures) and 912 m^2/g for the worm (wormhole shaped mesopores). Comparatively, sulfated zirconia (SZ) had a low BET surface area of only 63 m^2/g. The use of highly porous MCM-41 silica support to prepare mesoporous sulfated zirconia (MSZ) increased the surface area to 217 m^2/g. But this number was significantly less than the surface area reported by Sigma–Aldrich (approximately 1000 m^2/g) for unmodified MCM- 41 [15]. Deposition of zirconium oxide on MCM-41 may have blocked the pore openings reducing their volume. This was reflected in the pore volume of MSZ, which was only 0.15 cm^3/g compared with 0.96 cm^3/g for the unmodified MCM-41. Red mud measured an even lower surface area of 24 m^2/g but this was in the range reported in literature [27,28]. Commercially prepared HZSM-5, on the other hand, had a large surface area of 404 m^2/g. Compared to HZSM-5, where most of the porosity was contributed by micropores, the mesoporous MSU–S catalyst had very high porosity and hysteresis loops which are indicators of mesoporosity as shown in the comparison of nitrogen adsorption–desorption isotherms in Fig. 1. The MSU–S catalysts demonstrated isotherms of type II with the classical hysteresis loop of type H3 or H4, which is a characteristic of slit-shaped pores. The worm catalyst showed a hysteresis loop but also some capillary condensation at a high P/Po > 0.9 (Fig. 1). This is an indicator that large meso and macropores may exist due to the textural porosity provided by the worm-hole geometry [25]. The phenomenon was also observed in red mud which showed a sharp rise in adsorption at P/Po > 0.8. SEM micrographs of red mud have shown a range of particle sizes with different shapes and morphology, unlike HZSM-5 where the crystal size is uniform [17].

HZSM-5 had a median pore size of <1 nm while the mesoporous catalysts had pores between 2.4 and 3.5 nm. The mesoporous MSU–S catalysts had significantly higher pore volume ranging 0.96–1.49 cm^3/g compared with that for red mud, SZ and microporous HZSM-5 (0.24 cm^3/g). The large pore size of mesoporous catalysts is expected to reduce the diffusion resistance hindering the transport of large pyrolysis products such as anhydrosugars, phenolics, and lignin oligomers. Reactivity is expected to increase as more sites become available on the surface and in the mesopores [29].

Acidity is a strong indicator of a catalyst's activity and potential for transforming molecules through cracking and deoxygenation. HZSM-5 and SZ had a higher concentration of acid sites (>0.37 mmol/g, Table 1) when compared with the three mesoporous support based catalysts (<0.25 mmol/g). Although SZ is considered a superacid, its total acidity was measured lower than

Table 1
Comparison of catalyst properties.

Catalyst	Abbrev.	BET surface area (m^2/g)	Ext. surface area (m^2/g)	Pore size (nm)	Pore volume (cm^3/g)	Micropore vol. (cm^3/g)	Acid sites (mmol NH_3/g)
HZSM-5	–	404	135	0.6	0.25	0.121	0.40
SO_4^{2-} ZrO_2	SZ	63	61	3.6	0.08	0.001	0.37
SO_4^{2-} ZrO_2 MCM-41	MSZ	217	108	2.7	0.15	0.050	0.25
Al–MSU–S foam	Foam	995	NA	3.0	0.96	NA	0.21
Al–MSU–S worm	Worm	912	NA	3.5	1.49	NA	0.24
Red mud	RM	30	29	3.8	0.08	0.001	0.10

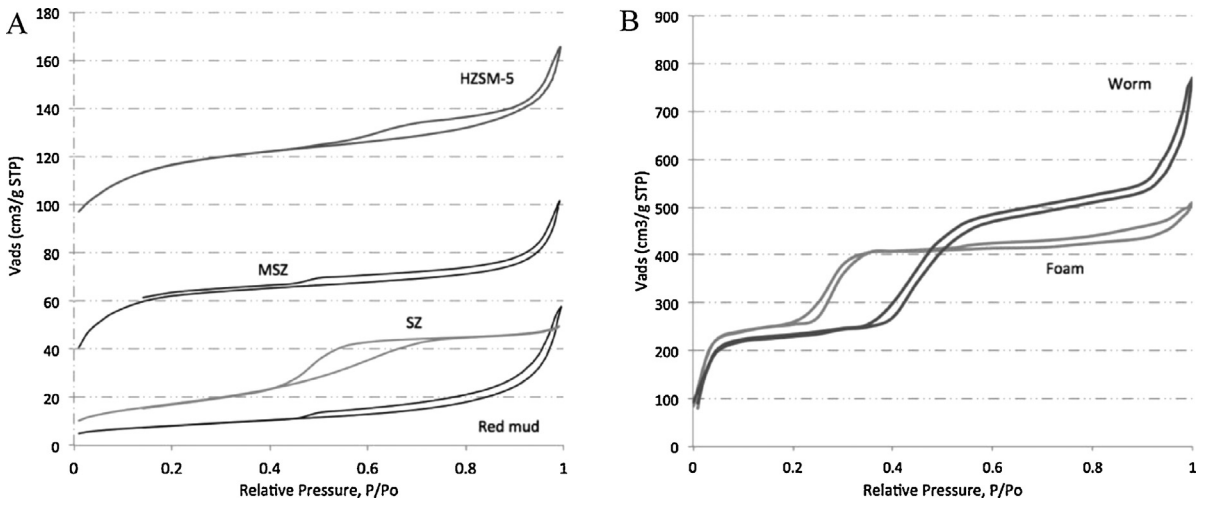

Fig. 1. Nitrogen gas adsorption–desorption isotherms for HZSM-5, sulfated zirconia (SZ), mesoporous sulfated zirconia (MSZ) and red mud catalysts (A); isotherms for mesoporous MSU–S catalysts, 2% Al–MSU–S worm and 2% Al–MSU–S foam (B).

with HZSM-5, as NH_3-TPD measurements were made below 700 °C. SZ has strongly bound acid sites that have been detected only at desorption temperatures of over 900 °C [14]. The mesoporous catalyst had a lower acidity compared to HZSM-5 and SZ due to lower crystallanity and mesopores, which reduced the concentration of active sites [25]. Despite containing metal oxides, red mud showed a reasonably high acidity of 0.10 mmol/g (though still lower than other catalysts), which has been attributed to the presence of Si–O–Al or Si–O–S units in its structure [28].

3.2. Pyrolysis–GC/MS

Experiments with the pyroprobe instrument used in this study were conducted with microgram samples of biomass packed between layers of quartz wool inside a quartz sample tube. Upon pyrolysis, volatile products are transported via a heated transfer line to the GC. Non-volatile products are left behind in the sample tube as char. For catalytic pyrolysis experiments, the catalyst was packed inside the sample tube such that the pyrolysis vapor reacted with the catalyst before exit to the transfer line and GC. Thus, much of the pyrolysis vapor cracked over the catalyst bed to produce smaller volatile fragments while the rest condensed on the catalyst surface as coke. Biomass pyrolysis alone produced many oxygenated and small molecules such as carbonyl and carboxyl group compounds, phenolics and anhydrosugars (Fig. 2). Very little hydrocarbons were produced. The use of a catalyst (HZSM-5, silica:alumina ratio, SAR = 23 in Fig. 2) deoxygenated these pyrolysis vapors to produce aromatics, light gases and coke. Carbon selectivity is defined as the moles of carbon in the product divided by the total moles of carbon in biomass. A comparison of products of HZSM-5 with the five non-zeolite catalysts is shown in Fig. 3, while the mass balance (quantitative comparison) is shown in Fig. 4. All catalysts reduced the condensable product yield due to thermal cracking of molecules, producing more non-condensable gas and coke. The carbon selectivity of catalytic pyrolysis products is shown in Fig. 5. The differences in chemical products and yields are discussed in the following sections.

3.2.1. Non-condensable gases

Catalysis increased the production of non-condensable gases, such as CO and CO_2, over biomass pyrolysis alone (Figs. 4 and 6). All catalysts produced similar gas yields in the range of 22–27% w/w biomass. Taarning et al. noted that alcohols and phenols lose oxygen in the form of H_2O, aldehydes and carbohydrates lose oxygen as CO and H_2O while carboxylic acids lose oxygen as CO_2 and H_2O. All of the catalysts produced greater than 8.5% w/w biomass of CO (Fig. 5). Although HZSM-5 removed more oxygenates than other catalysts, mesoporous MSZ and worm catalyst produced the most CO (Fig. 6). Of the six catalysts, red mud generated the most CO_2 (~13–15% of biomass weight). The cracking activity of red mud is due to the presence of silica and alumina which provide the acidic functionality [17,19]. CO_2 yields have been related to Al content in the catalyst which enhances the decarboxylation reactions by Bronsted acid catalysis [20]. Indeed, no carboxyl group compounds such as acetic acid, a major product of biomass pyrolysis, were detected after red mud catalysis. The silica:alumina ratio (SAR) in red mud is <1.3, which is very low compared to other catalysts such as HZSM-5 (SAR = 23). Red mud had much higher Al content compared to all other catalysts and produced more CO_2 from the decarboxylation of acids in the pyrolysis product [19]. Thus, red mud may be used as an inexpensive catalyst to remove corrosive acids and upgrade pyrolysis vapor. In the process, highly alkaline red mud is itself reduced to a magnetic, non-alkaline iron ore resource [27,30].

For the sulfated zirconia catalyst, evolution of carbon oxides was accompanied by SO_2 (Fig. 3). The presence of SO_2 has been linked to the reaction of carbon atoms with oxygen atoms from the surface sulfate groups to form carbon oxides [31]. A large quantity of oxygenates, carbon oxides and SO_2 in the products of SZ pyrolysis indicate that carbon from coke may have reacted with the catalyst surface, producing carbon oxides and SO_2, resulting in a loss in catalytic activity.

3.2.2. Solid product: char and coke

Biomass pyrolysis followed by catalysis generated large quantities of carbonaceous solid residues in the form of char and coke. In the present study, biomass samples were separated from the catalyst to simulate pyrolysis followed by a separate catalysis step. Thus, biomass pyrolyzed to char and vapor before reacting over the catalyst. Reactions of the pyrolysis vapors over the catalyst produced solid coke. Char and coke in this study could not be measured separately and hence are reported as one combined value. The mesoporous catalysts produced more char and coke; 38% w/w biomass for MSZ and worm, 49% for foam, and 34–36% for HZSM-5, SZ and red mud (Fig. 4).

The char yield is consistent for all catalyst experiments as biomass pyrolysis occurs first and the vapors produced then diffuse and react over the catalyst bed. Therefore, the difference in yield between catalysts is attributed to coking during the catalyst

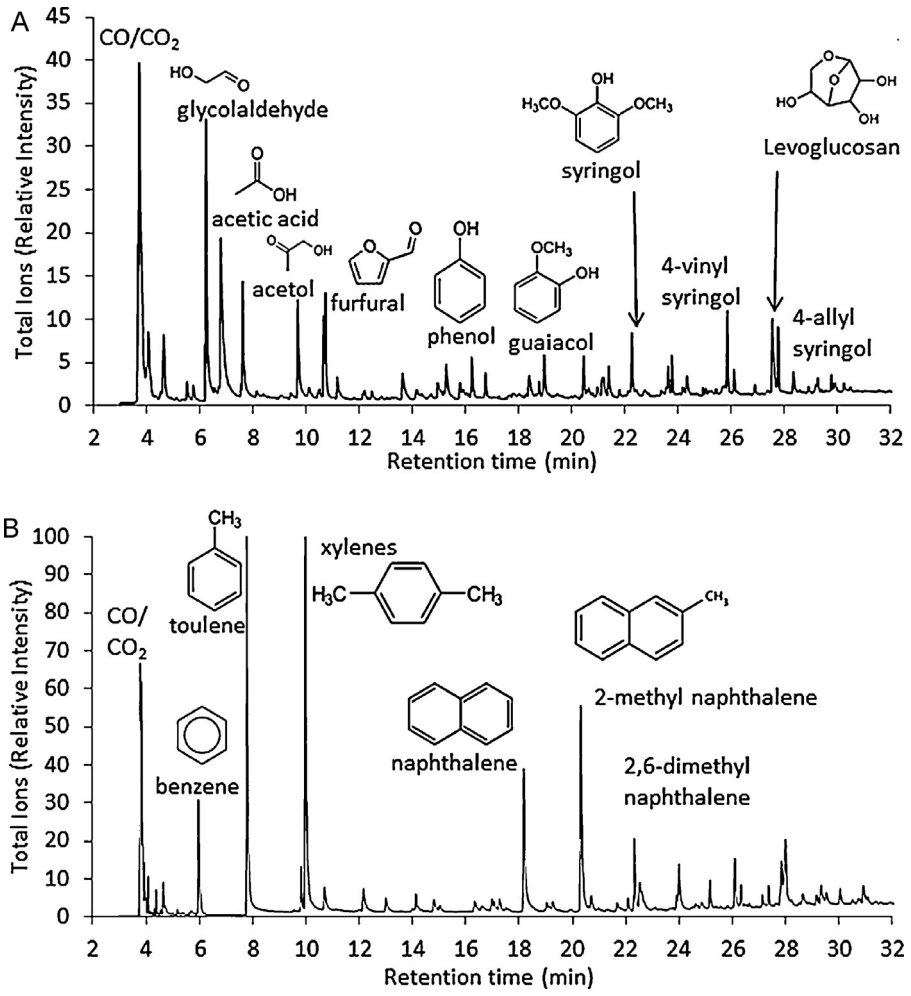

Fig. 2. A: comparison of GC/MS chromatograms from pyrolysis of poplar (A) and catalytic pyrolysis with HZSM-5 (silica:alumina ratio: 23) (B).
List of non-condensables quantified (using Agilent CP-Porabond Q column):
Methane, carbon monoxide, carbon dioxide, ethylene, ethane, methyl alcohol, propene, propane, propylene, dimethyl ether, isobutane, butene, butane, sulfur dioxide.
List of condensables quantified (using Restek Rtx-1701 column):
Acetaldehyde, 2-propenal, furan, acetone, ammonium acetate, hydroxyacetaldehyde, acetic acid methyl ester, 2,3-butanedione, 2-methyl-furan, 1-hydroxy-2-propanone, 2-butenal, benzene, acetic acid, furfural, toluene, hexanal, 2-cyclopentene-1,4-dione, cyclohexanone, 2-furanmethanol, 2-methyl-2-cyclopenten-1-one, *p*-xylene, styrene, *o*-xylene, 2-methylphenol, 1-ethyl-2-methyl-benzene, 3-methyl-phenol, 1,2,4-trimethyl-benzene, indane, indene, octanal, 2-methyl-benzofuran, 2-methylindene, naphthalene, 2,6-dimethoxy-phenol, 2-methylnaphthalene, 1,2,3-trimethoxybenzene, 2,6-dimethylnaphthalene.

reaction only. Highly acidic catalysts are good cracking catalysts and prone to heavy coke generation [20,32]. Therefore, it was surprising that the superacid sulfated zirconia catalyst produced the least char and coke (34.5%). SZ also has a low resistance to coke and produced the highest amount of carbon oxides. Coke deposited on SZ surfaces may have reacted with oxygen atoms from the surface sulfate groups to form carbon oxides [31]. This explains why the coke yield decreased while the amount of carbon oxides, sulfur oxides and other oxygenates in the vapor product increased.

In microporous catalysts such as HZSM-5, there are often diffusion limitations due to formation of coke molecules on the surface or in pores that block the reactant from accessing the active sites [33]. Phenolics that are larger than the pore size of HZSM-5 remain unconverted or produce molecules that are precursors to coke generation [34–36]. Once the coke precursors are generated, they are retained on the catalyst by steric hindrance, strong chemisorption or low volatility [10,32]. Steric hindrance occurs due to differences between the average pore diameter and pore opening or aperture size. Large pores and their intersections, known as channel intersections, are also sites for coke formation [10]. MSU–S catalysts have strong acid sites that can reduce hydrocarbons to non-condensable gases and coke precursor molecules. The large mesopores enable production of undesirable polyaromatic hydrocarbons (PAH) leading to coke formation through condensation and polymerization reactions [11,32,35]. Thus, although mesoporous catalysts have large pores that help diffusion, high acidity combined with steric hindrance also promotes coke production.

The pyroprobe has been successfully used as a screening tool even though it is a batch reactor and the amount of char produced is greater than in bench-scale or fluidized bed experiments [37,38]. In continuous bench or larger scale experiments, char would be generated in the pyrolysis reactor and continuously removed while coke would generate and accumulate on the catalyst surface. Catalyst coking is pronounced in the beginning and the rate of coke generation decreases swiftly with time on stream, [39–41]. Additionally, a large fraction (>90%) of total coke is classified as "soluble" coke, which is continuously thermally disintegrated, especially at reaction temperatures of 500–550 °C [42,43]. The remaining is "insoluble" coke that deposits on the external surface and inside the pores, where strong acidic sites with small apertures or cages exists [35,44]. Thus, in a scaled-up continuous process, much of the soluble coke will be continuously removed from the catalyst surface, ensuring longer catalyst active time before regeneration is required.

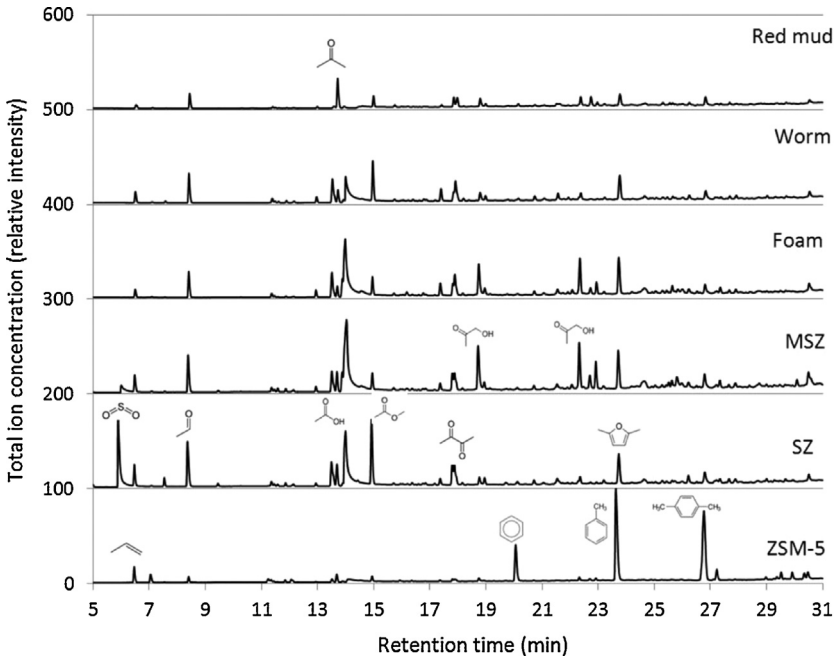

Fig. 3. Representative pyrogram for catalytic pyrolysis of poplar with catalysts as analyzed by an Agilent CP-Porabond Q column. HZSM-5 catalyst had a silica:alumina ratio of 23.
Note: chromatograms are offset by 100 data points on the *Y*-axis for clarity.

Deactivation of zeolite catalyst (SAR = 23) was tested in a continuous experiment where biomass pyrolysis vapors were fed over a fixed bed catalytic reactor. Preliminary results showed that deactivation (loss of aromatics generation) was observed after feedstock equal to 20 times the catalyst weight was processed. Coke generated was approximately 8% of catalyst mass, similar to observations made by Valle et al. [42]. Upon deactivation, the catalyst was regenerated and re-used several times for the pyrolysis process without significant loss of activity [38].

3.2.3. Condensable fraction: aromatics and oxygenates

A number of oxygenated molecules (condensable fraction which includes aldehydes, ketones, acids etc., but not including phenolics) were produced upon poplar pyrolysis and accounted for 23 ± 1.4% of the original carbon in biomass (Fig. 5). Many of these oxygenated molecules such as acetic acid and its derivatives, acetol, acetaldehyde and 2,5-dimethylfuran remained unreacted over the non-zeolite catalysts, especially sulfated zirconia. The mesoporous MSU–S and MSZ catalysts deoxygenated the pyrolysis vapor but more than 8% of the biomass carbon was still observed in the form of oxygenates. Despite its high acidity, the SZ catalyst was the least effective with over 17% of the carbon still present in the form of volatile oxygenates. Sulfated zirconia has been known to have a low tolerance for coking and much of its catalyst activity may have been quickly lost due to coke deposition [45]. HZSM-5 and red mud were the most effective; oxygenates accounted for <2% of original biomass carbon for HZSM-5 and approximately 3.5% for red mud. Due to the differences in density of the various catalysts in this study and the small sample tube, the catalyst to biomass ratio used in these experiments was only 5:1. This is much lower than the 10

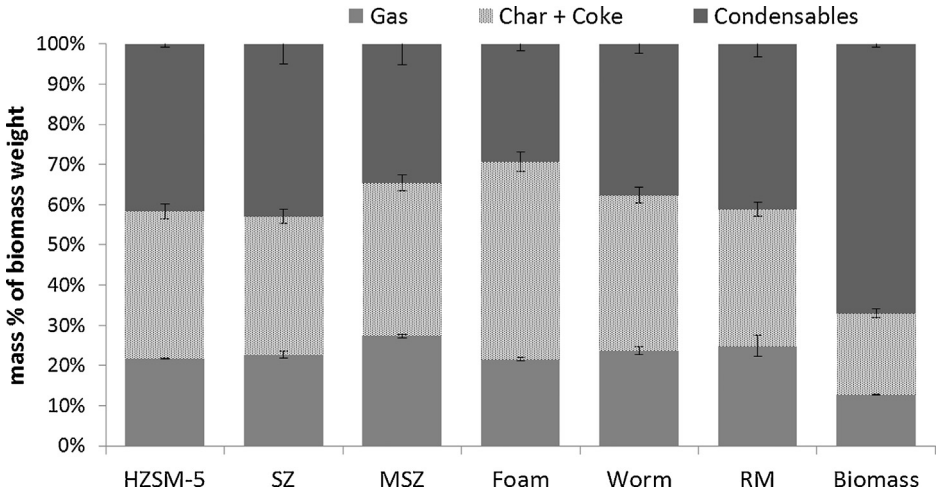

Fig. 4. Mass balance for poplar catalytic fast pyrolysis in Py–GC/MS. Condensable fraction includes GC detectable compounds, water as well as those compounds not detected by GC analysis and was obtained from difference. Solid content was obtained from weighing of samples before and after pyrolysis while the gas content was determined from quantification. Carbon balance (Fig. 5) showed that greater than 95% of the biomass carbon was detected in the products for catalytic pyrolysis. Biomass refers to neat biomass pyrolyzed without catalyst. Only char was produced for biomass (poplar DN-34) pyrolysis. HZSM-5 catalyst had a silica:alumina ratio of 23.

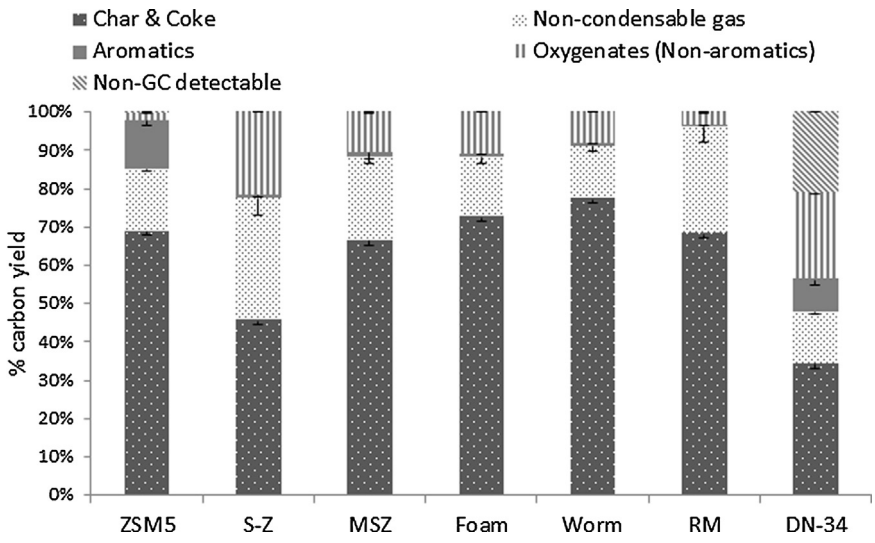

Fig. 5. Carbon yield for poplar catalytic fast pyrolysis in Py–GC/MS. HZSM-5 catalyst had a silica:alumina ratio of 23. DN-34 refers to pyrolysis of neat poplar biomass without catalyst.

or 19:1 ratios used in other analytical pyrolysis studies and may be one of the reasons for the incomplete removal of oxygenates [38,46].

"Aromatics" refers to aromatic hydrocarbons and phenolic molecules. Non-catalytic biomass pyrolysis products contained negligible hydrocarbons but a significant amount of phenolics from lignin pyrolysis. The following major lignin derivatives were observed: phenol, 2,6-dimethoxyphenol, 4-methylsyringol, 4-vinylsyringol, 4-allylsyringol, trimethoxybenezene derivatives and methoxybenzaldehydes. In the absence of a catalyst, less than 8% of biomass carbon was observed as aromatics, mostly phenolics (Fig. 5). The mesoporous and sulfated zirconia catalysts did not produce aromatic hydrocarbons and less than 1% of the biomass carbon was observed as aromatics. Some aromatics such as methoxybenzaldehydes, syringol and indene were found in the product stream. Although the total aromatic yield from red mud catalysis was low (<1%), a variety of molecules including the hydrocarbons toluene and *p*-xylene were observed along with phenolics. On the other hand, in catalytic pyrolysis with HZSM-5, over 13% of the carbon was found in aromatic molecules, of which the C6–C8 monoaromatics such as *p*-xylene were a large fraction. Aromatics such as syringol, 4-allylsyringol, trimethoxybenezene derivatives and methoxybenzaldehydes were also present. The yield of phenolics from catalytic pyrolysis was small compared with non-catalytic biomass pyrolysis. The difference may be attributed to either conversion of guaiacyls/syringols to non-phenolic aromatics or to their conversion to coke on the catalyst surface [22,34,47].

MSU–S catalysts produced less aromatics than HZSM-5. High-angle X-ray diffraction of MSU–S catalysts has shown the absence of Braggs peaks and crystallite phases, present in HZSM-5, that may be responsible for its shape selectivity and high aromatics production [24,25] . Jae et al. studied the kinetic diameters of benzene and *p*-xylene and observed that they were closest to the pore dimensions of HZSM-5 [10]. They noted the importance of pore window size, internal pore space and steric hindrance in determining aromatic production and showed that large pores facilitated coke formation.

To summarize, mesoporous catalysts in the present study had many desirable properties such as mesoporosity, high pore volume or acidity. However, a combination of high acidity and large pores induced cracking of pyrolysis products leading to greater production of non-condensable gases and coke [11,32]. Oxygen from biomass pyrolysis vapor was removed as carbon oxides. Thus,

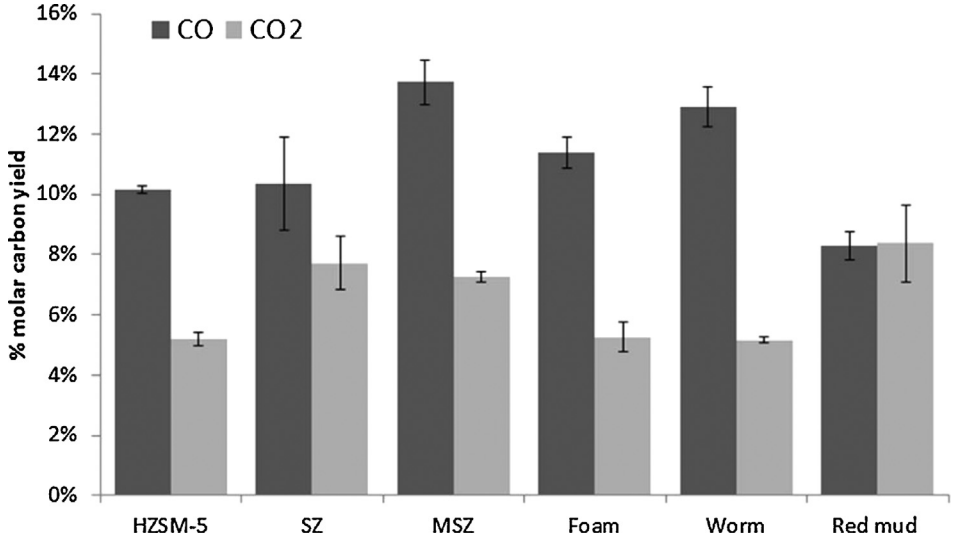

Fig. 6. Production of carbon oxides from pyrolysis with different catalysts.

catalysts other than HZSM-5 were effective in deoxygenation but were not selective to aromatics. Our experiments show that HZSM-5, or other such zeolite catalysts with tunable porosity, exhibit increased yields of aromatics.

3.3. Comparison of HZSM-5 with varying acidity

HZSM-5 is a crystalline aluminosilicate zeolite with a high silica and low aluminum content. The increase in aluminum content of HZSM-5 increases its Bronsted acid sites. With change in the concentration and strength of active sites, an effect on yields of aromatics is to be expected. For comparison of HZSM-5 catalysts with different silica–alumina content, catalytic pyrolysis experiments were conducted with ground poplar wood under identical conditions described in the Section 2. The products of biomass pyrolysis are compared with catalytic pyrolysis in the presence of HZSM-5 in Fig. 2. These experiments differ from a study by Foster et al. who compared four HZSM-5 catalysts for glucose pyrolysis, while in the present study, lignocellulosic biomass is tested with five varieties of HZSM-5. Sample preparation also differed as Foster et al. did their experiments by preparing very small particle size (<250 μm) mixtures of glucose and catalyst, whereas in the current study, biomass (1 mm) was packed between layers of quartz wool and catalyst to simulate pyrolysis followed by catalysis [20]. While Foster et al. observed the highest aromatic yields and lowest coke for the catalyst with silica alumina ratio (SAR) of 30 [20] for glucose mixtures, our experiments with biomass did not show significant differences ($p < 0.05$) between catalysts with SAR of 23 and 30 (Figs. 7 and 8).

Aromatic selectivity is defined as the moles of carbon in the product divided by the total moles of carbon in all aromatic molecules. SAR23 produced greater amounts of small aromatics such as C6 (benzene) and C7 (toluene and methylphenols) while SAR30 produced larger quantities of C8 and C9 aromatics. SAR23, with the highest concentration of acidic sites, also produced the most C10+ polyaromatics and coke, for which polyaromatics are precursors. The C8 and C9 selectivity increased with SAR suggesting that a lower concentration of acidic sites tends to produce greater amount of xylenes and tri-methylbenzene molecules [20]. SAR23 almost completely eliminated oxygenated molecules from the product and the conversion to aromatics decreased with decrease in acidity and increase in SAR. SAR280 was particularly selective toward production of C9+ monoaromatics but not selective for C10+ polyaromatics such as naphthalenes. As a result of its large yield of C9 aromatics, SAR280 showed greater carbon selectivity for total aromatics over SAR55 and 80.

The non-condensable gases, CO and CO_2, are considered to be the products of decarbonylation and decarboxylation reactions, respectively [20,36]. The non-condensable gas yield decreased with increasing SAR, although it was not significantly different between SAR23 and 30 (Fig. 9). SAR30 produced the highest CO but was similar ($p > 0.05$) to SAR23, which produced the most CO_2. Foster et al. have proposed that CO_2 production may be related to aluminum content in the catalyst as decarboxylation is enhanced by Bronsted acid catalysis [20]. This was observed in the present study as well, where the CO_2 production decreased with increasing SAR. SAR23 and 30 both generated alkanes and alkenes as non-condensable gas. The char and coke carbon yields were not significantly different between the five zeolites but showed a decreasing trend with increase in SAR. At low SAR, the concentration and the acid strength of active sites increases, leading to greater cracking and secondary reactions that generate more reactive molecules and coke [35]. These results show that high acidity, low SAR, HZSM-5 (SAR23 and 30) needs to be employed to increase yield of total aromatics, especially BTEX, from biomass pyrolysis. Selectivity for C8 and C9 monoaromatics such as *p*-xylene, however, may be increased by using a catalyst with higher SAR (>50).

3.4. Reaction pathways to aromatics over HZSM-5

Pyrolysis thermally decomposes biomass into smaller oxygenated molecules such as carbon oxides, alcohols, aldehydes, ketones, phenolics and anhydrosugars (Fig. 2). These intermediate oxygenates then diffuse into the pores of a catalyst where they are broken down into smaller dehydrated molecules [49] . Park et al. concluded that the pathway intermediates to aromatics are always C_2–C_4 olefins irrespective of the number of carbon atoms in the feed [6]. Therefore, once dehydrated species are produced, it would be necessary for these intermediates of different carbon lengths to go through the olefin to aromatics route via C_2–C_4 hydrocarbon fragments that form the 'hydrocarbon pool' (Fig. 10) [50]. The hydrocarbon pool may consist of polymethylbenzene, benzenium cations, carbenium ions or naphthenes in pseudo-equilibrium [3,51–53] . The kinetic diameters of molecules present in the reactive hydrocarbon pool is between 5.7 and 6.0 Å, similar to the pore size of HZSM-5 catalyst as well as the kinetic diameters of benzene, indene, 2-furanmethanol and 4-methylfurfural [10,54].

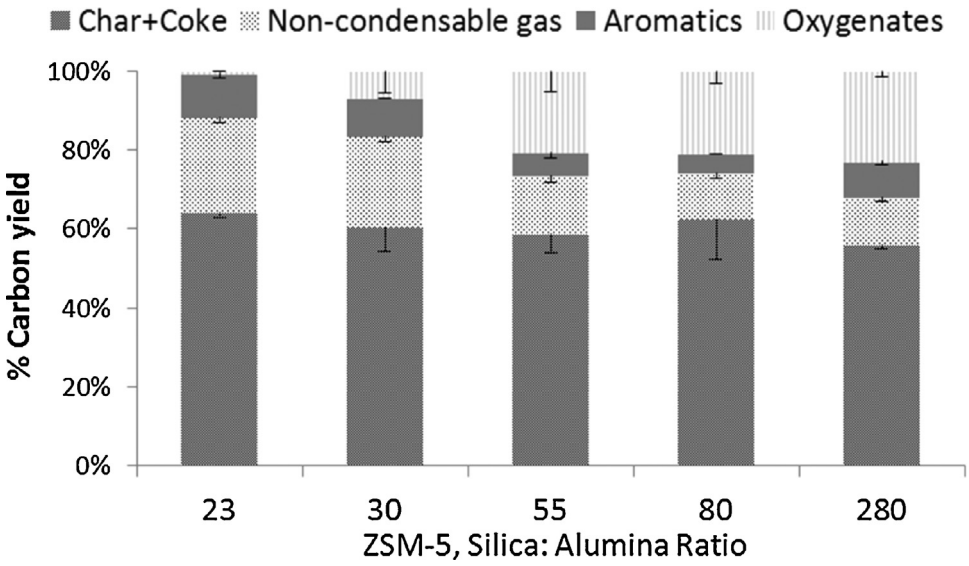

Fig. 7. Carbon balance of catalytic biomass pyrolysis with HZSM-5 at different SAR.

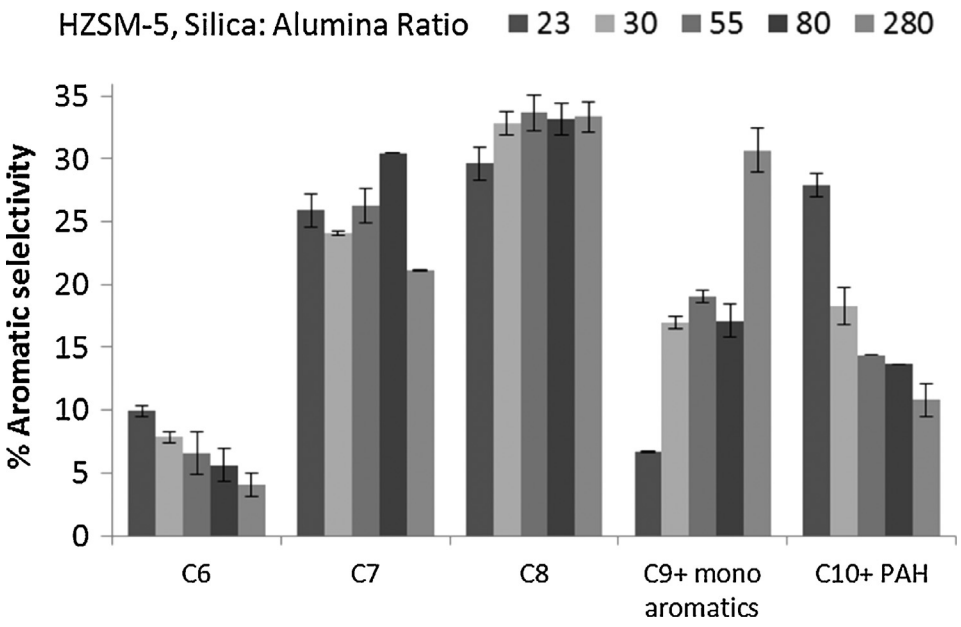

Fig. 8. Aromatic selectivity of HZSM-5 at different SAR.

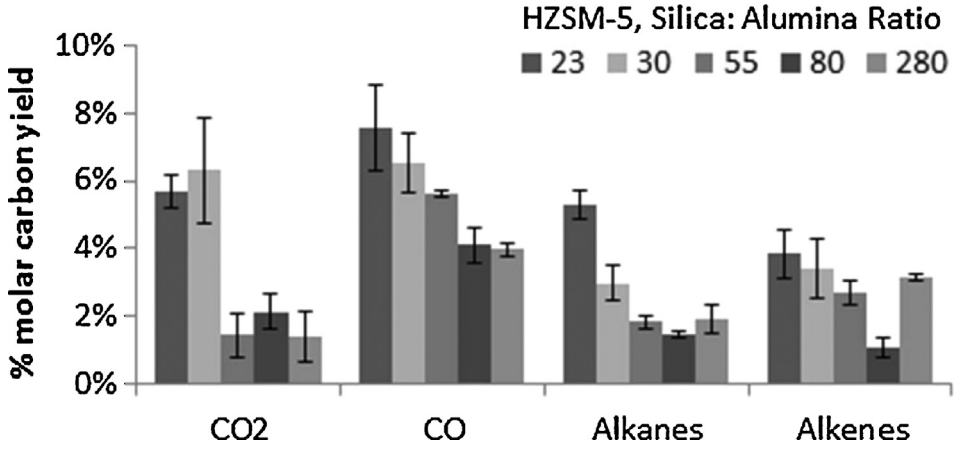

Fig. 9. Gas composition of products of HZSM-5 catalytic pyrolysis.

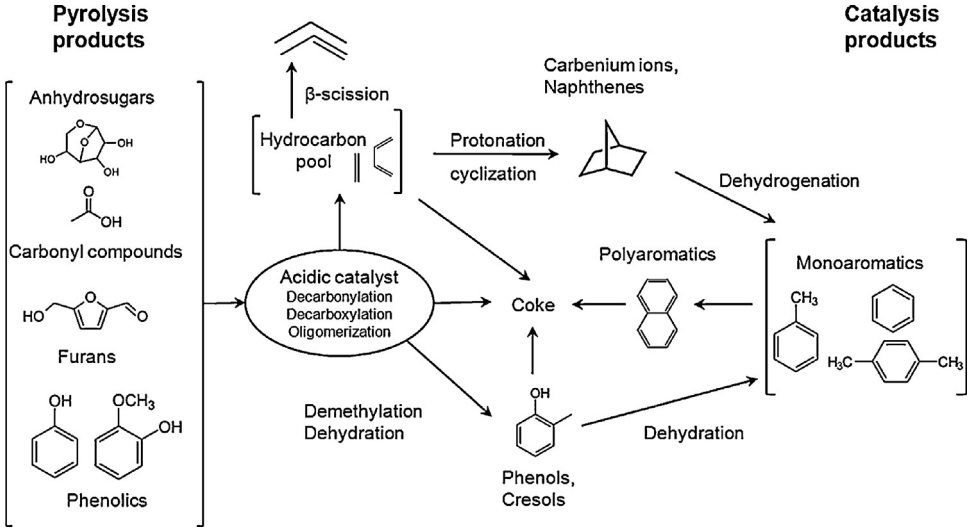

Fig. 10. Proposed pathways for cellulose to aromatics [6,38,53,58].

The combination of appropriately sized crystalline micropores and high acidity makes HZSM-5 ideal for producing monoaromatic molecules such as BTEX. Monocyclic aromatics and their reaction with other oxygenates leads to the production of naphthalenes and other polycyclic aromatics.

Besides aromatics, HZSM-5 produces significant coke as well. Aromatics and coke production from acid catalyzed polymerization of oxygenates such as furans have been observed as competing reactions [55,56]. Olefins are precusors to producing aromatic molecules and many studies have shown that increasing the olefin content in feed increases the aromatics in catalysis products [6,38,57,58]. At the same time, olefins can also increase coke production as highly acidic catalysts are more selective toward cracking to produce light gases and coke precursors through β-scission [53,59]. This explains why catalysts like SAR23 with a high concentration of acid sites have a greater tendency for producing both aromatics and coke.

Many groups have studied the reactions of specific pyrolysis products over zeolite catalysts. Alcohols undergo dehydration at low temperatures (<250 °C) to form olefins, which are converted into alkanes and aromatics at higher temperatures [34]. Acetaldehyde forms significant amounts of coke; acetone converts to isobutene, heavier olefins, aromatics and alkanes at higher temperatures; while oxygen from carboxylic acids is removed as CO_2 [36,57]. Further, phenolic compounds produce more coke than non-phenolic molecules [2,36]. Highly acidic sites present inside HZSM-5 pores are necessary to crack lignin derivatives into the olefins and allenes needed for aromatics production [22]. But these sites are not accessible to many phenolic compounds due to differences in their kinetic diameter and catalyst pore size [22,47,60]. Therefore, they do not decompose significantly to produce aromatics and instead contribute to coke production. These studies suggest that removal of aldehydes and phenolics from the pyrolysis oil before zeolite catalysis will reduce coking while carboxylic acids may be desired to increase H/C ratio in pyrolysis vapor and for hydrocarbon generation [60].

4. Conclusions

Our experiments show that microporous HZSM-5 catalysts provide the desired shape selectivity and acidity to produce aromatics from pyrolysis of biomass, a renewable resource. In particular, zeolite catalysts have been shown to be effective at temperatures modest for thermochemical conversion of biomass, at low pressure, and in the absence of molecular hydrogen as a co-feed. The silica-alumina ratio in HZSM-5 affects the aromatic product distribution and yield. SAR 23 and 30 gave the highest aromatic yields from actual lignocellulosic biomass. The yields from catalytic pyrolysis of biomass are lower than those obtained when neat compounds such as glucose or cellulose are used as feedstock [4,20,23]. Therefore, significant potential exists for improving product yield from zeolite catalysts such as HZSM-5 by altering the pore structure and adding catalyst promoters and modifiers [6,10,16,44,61].

Aromatics and coke production are both functions of catalyst acidity, shape selectivity and pore size. Mesoporous catalysts such as Al–MSU–S foam and worm removed diffusion resistance and provided a high deoxygenating activity. However, due to absence of crystalline micropores and presence of large pores, the mesoporous catalysts were not selective to hydrocarbon aromatics. Although sulfated zirconia is a superacid, it was not shape selective to aromatic molecules and produced coke. Synthesis of sulfated zirconia on a mesoporous MCM-41 support was demonstrated. This mesoporous sulfated zirconia showed an increased surface area, improved deoxygenating activity and stability to coking, which opens up new avenues for using this highly acidic catalyst. Red mud, a highly alkaline industrial waste, demonstrated significant decarboxylating activity. Its use in biomass pyrolysis offers the potential benefit of upgrading two low value resources, biomass and red mud, into higher value products. The non-zeolitic catalysts in this study were not selective to aromatic molecules. However, they demonstrated significant deoxygenating activity and may be useful for other applications including upgrading of pyrolysis vapor for producing biofuels.

Acknowledgments

The authors thank The Coca-Cola Company for providing financial support. Thanks also to Professor Marcel Schlaf and Dr Elham Karimi from the University of Guelph, ON, Canada, for providing samples of red mud and Ms. Kris Van Winkle for technical support and instrument maintenance.

References

[1] N.Y. Chen, T.F. Degnan, L.R. Koenig, Chemtech 16 (1986) 506.
[2] P.T. Williams, P.A. Horne, J. Anal. Appl. Pyrol. 31 (1995) 39.
[3] J.P. Diebold, J. Scahill, ACS Div. Fuel Chem. 32 (1987) 297.
[4] J.D. Adjaye, N.N. Bakhshi, Fuel Process. Technol. 45 (1995) 185.
[5] B. Valle, A.G. Gayubo, A. Alonso, A.T. Aguayo, J. Bilbao, Appl. Catal. B Environ. 100 (2010) 318.
[6] H.J. Park, H.S. Heo, J.-K. Jeon, J. Kim, R. Ryoo, K.-E. Jeong, Y.-K. Park, Appl. Catal. B Environ. 95 (2010) 365.
[7] E.F. Iliopoulou, S.D. Stefanidis, K.G. Kalogiannis, A. Delimitis, A.A. Lappas, K.S. Triantafyllidis, Appl. Catal. B Environ. 127 (2012) 281.
[8] C.M. Lew, R. Cai, Y. Yan, Acc. Chem. Res. 43 (2010) 210.
[9] S. Kelkar, Z. Li, J. Bovee, K.D. Thelen, R.M. Kriegel, C.M. Saffron, Biomass Bioenergy 64 (2014) 152.
[10] J. Jae, G.A. Tompsett, A.J. Foster, K.D. Hammond, S.M. Auerbach, R.F. Lobo, G.W. Huber, J. Catal. 279 (2011) 257.
[11] K.S. Triantafyllidis, E. Iliopoulou, E. Antonakou, A. Lappas, H. Wang, T.J. Pinnavaia, Microporous Mesoporous Mater. 99 (2007) 132.
[12] E. Ghedini, M. Signoretto, F. Pinna, G. Cruciani, Catal. Lett. 125 (2008) 359.
[13] H. Ohtsuka, T. Tabata, T. Hirano, Appl. Catal. B Environ. 28 (2000) L73.
[14] Y. Sun, L. Zhu, H. Lu, R. Wang, S. Lin, D. Jiang, F. Xiao, Appl. Catal. 237 (2002) 21.
[15] A. Pattiya, J.O. Titiloye, A.V. Bridgwater, Fuel 89 (2010) 244.
[16] J. Adam, E. Antonakou, A. Lappas, M. Stöcker, M.H. Nilsen, A. Bouzga, J.E. Hustad, G. Øye, Microporous Mesoporous Mater. 96 (2006) 93.
[17] A. Lopez, I. de Marco, B.M. Caballero, M.F. Laresgoiti, A. Adrados, A. Aranzabal, Appl. Catal. B Environ. 104 (2011) 211.
[18] M. Balakrishnan, V.S. Batra, J.S.J. Hargreaves, A. Monaghan, I.D. Pulford, J.L. Rico, S. Sushil, Green Chem. 11 (2009) 42.
[19] E. Karimi, A. Gomez, S.W. Kycia, M. Schlaf, Energy Fuels 24 (2010) 2747.
[20] A.J. Foster, J. Jae, Y.-T. Cheng, G.W. Huber, R.F. Lobo, Appl. Catal. A Gen. 423–424 (2012) 154.
[21] T.R. Carlson, G. a. Tompsett, W.C. Conner, G.W. Huber, Top. Catal. 52 (2009) 241.
[22] C.A. Mullen, A.A. Boateng, Fuel Process. Technol. 91 (2010) 1446.
[23] J.D. Adjaye, N.N. Bakhshi, Biomass Bioenergy 7 (1994) 201.
[24] Y. Liu, W. Zhang, T.J. Pinnavaia, Angew. Chem. Int. Ed. 40 (2001) 1255.
[25] Y. Liu, T.J. Pinnavaia, J. Mater. Chem. 14 (2004) 1099.
[26] ASTM International, ASTM D4442 – 07 ASTM Int. (2007).
[27] S. Sushil, A.M. Alabdulrahman, M. Balakrishnan, V.S. Batra, R.A. Blackley, J. Clapp, J.S.J. Hargreaves, A. Monaghan, I.D. Pulford, J.L. Rico, W. Zhou, J. Hazard. Mater. 180 (2010) 409.
[28] S. Wang, H.M. Ang, M.O. Tadé, Chemosphere 72 (2008) 1621.
[29] G. Fogassy, N. Thegarid, Y. Schuurman, C. Mirodatos, Energy Environ. Sci. 4 (2011) 5068.
[30] E. Karimi, C. Briens, F. Berruti, S. Moloodi, T. Tzanetakis, M.J. Thomson, M. Schlaf, Energy Fuels 24 (2010) 6586.
[31] B. Li, R.D. Gonzalez, Appl. Catal. A Gen. 165 (1997) 291.
[32] M. Guisnet, P. Magnoux, Appl. Catal. A Gen. 212 (2001) 83.
[33] I. Graça, J.M. Lopes, M.F. Ribeiro, F. Ramôa Ribeiro, H.S. Cerqueira, M.B.B. de Almeida, Appl. Catal. B Environ. 101 (2011) 613.
[34] A.G. Gayubo, A.T. Aguayo, A. Atutxa, R. Aguado, J. Bilbao, M. Olazar, Ind. Eng. Chem. Res. 43 (2004) 2610.
[35] M. Guisnet, L. Costa, F.R. Ribeiro, J. Mol. Catal. A Chem. 305 (2009) 69.
[36] E. Taarning, C.M. Osmundsen, X. Yang, B. Voss, S.I. Andersen, C.H. Christensen, Energy Environ. Sci. 4 (2011) 793.
[37] E. Biagini, F. Lippi, L. Tognotti, Fuel 85 (2006) 2408.
[38] T.R. Carlson, Y.-T. Cheng, J. Jae, G.W. Huber, Energy Environ. Sci. 4 (2011) 145.
[39] A.A. Brillis, G. Manos, Ind. Eng. Chem. Res. 42 (2003) 2292.
[40] P. Magnoux, M. Guisnet, Zeolites 9 (1989) 329.
[41] B. Wang, Ph.D. Dissertation, University College London, 2007, 2015.
[42] B. Valle, P. Castaño, M. Olazar, J. Bilbao, A.G. Gayubo, J. Catal. 285 (2012) 304.

[43] P. Turlier, M. Forissier, P. Rivault, I. Pitault, J.R. Bernard, in: M.L. Occelli, P. O'Connor. American Chemical Society, Washington, DC (1994).
[44] G.T. Neumann, J.C. Hicks, ACS Catal. 2 (2012) 642.
[45] B. Li, R.D. Gonzalez, Appl. Catal. A Gen. 174 (1998) 109.
[46] S. Thangalazhy-Gopakumar, S. Adhikari, R.B. Gupta, Energy Fuels 26 (2012) 5300.
[47] V. Srinivasan, S. Adhikari, S.A. Chattanathan, S. Park, Energy Fuels 26 (2012) 7347.
[49] T.R. Carlson, J. Jae, G.W. Huber, ChemCatChem 1 (2009) 107.
[50] M. Stöcker, Microporous Mesoporous Mater. 29 (1999) 3.
[51] J.F. Haw, W. Song, D.M. Marcus, J.B. Nicholas, Acc. Chem. Res. 36 (2003) 317.
[52] M. Bjorgen, S. Svelle, F. Joensen, J. Nerlov, S. Kolboe, F. Bonino, L. Palumbo, S. Bordiga, U. Olysbye, J. Catal. 249 (2007) 195.
[53] C. Liu, Y. Deng, Y. Pan, Y. Gu, B. Qiao, X. Gao, J. Mol. Catal. A Chem. 215 (2004) 195.
[54] Q. Wang, Z. Cui, C. Cao, W. Song, J. Phys. Chem. C 115 (2011) 24987.
[55] M. Choura, N.M. Belgacem, A. Gandini, Macromolecules 29 (1996) 3839.
[56] S. Bertarione, F. Bonino, F. Cesano, A. Damin, D. Scarano, A. Zecchina, J. Phys. Chem. B 112 (2008) 2580.
[57] P.A. Horne, N. Nugranad, P.T. Williams, J. Anal. Appl. Pyrol. 34 (1995) 87.
[58] M. Tagliabue, A. Carati, C. Flego, R. Millini, C. Perego, P. Pollesel, B. Stocchi, G. Terzoni, Appl. Catal. A Gen. 265 (2004) 23.
[59] R. Fricke, H. Kosslick, G. Lischke, M. Richter, Chem. Rev. 100 (2000) 2303.
[60] A.G. Gayubo, A.T. Aguayo, A. Atutxa, R. Aguado, M. Olazar, J. Bilbao, Ind. Eng. Chem. Res. 43 (2004) 2619.
[61] S. Kelkar, C.M. Saffron, Z. Li, S.-S. Kim, T.J. Pinnavaia, D.J. Miller, R. Kriegel, Green Chem 16 (2014) 803.